1.33 Enhanced Photocatalytic Activity for H_2 Production by RGO/P25 Composite through UV Assisted Anchoring

B. C. Hernández-Majalca, M.J. Melendez-Zaragoza, J.M. Salinas-Gutiérrez, A. López-Ortiz, V. Collins-Martínez

Laboratorio Nacional de Nanotecnología Centro de Investigación en Materiales Avanzados, S. C. Chihuahua, Chih., México
* Corresponding author: virginia.collins@cimav.edu.mx

ABSTRACT

In this work, graphene oxide (GO) was prepared by the Tour method from graphite powder employing a microwave pre-treatment, which was used to modify TiO_2 (P25). A composite of reduced graphene oxide (RGO) and P25 was prepared (RGO/P25) by UV assisted anchoring of P25 on RGO. The structure, morphology, textural and optical properties were studied by XRD, SEM, BET and UV-Vis techniques, respectively. Water splitting photocatalytic evaluation used an aqueous methanol solution of the suspended composite material and a 250 W mercury lamp as light irradiation source. Results indicate a bandgap value of 2.57 eV for the RGO/P25 composite, while this material exhibited a H_2 production rate greater than either P25 or graphene oxide alone. A significant enhancement in the hydrogen production rate was achieved by RGO/P25 as photocatalyst obtaining ~400 µmol H_2/gh. This can be presumably attributed to graphene oxide acting as an electron collector and transporter in the RGO/P25 composite.

Keywords: graphene oxide, anchorage UV-assisted, Photocatalysis, hydrogen production.

Introduction

Globally, the demand for energy in the coming years will considerably increase. An ideal alternative, already considered, is solar energy becoming the most powerful, accessible as far as "cost" is concerned, as well as the richest source of renewable and sustainable energy [1].

Furthermore, hydrogen has a high specific energy density and its combustion generates only water as a by-product, which makes H_2 an attractive carbon free fuel. Despite the fact that hydrogen in its elemental form is not very abundant in the environment, this is offset by its abundant natural source (water molecule) the obtaining of this fuel and the combination of the use of solar technologies, makes it possible to cover the global demand for energy in an environmentally friendly manner.

Nowadays, there is a variety of methods used to produce hydrogen by water splitting using solar radiation [2], [3]; photovoltaic electrolysis of water by proton exchange membranes [4] and alkaline electrolytes [5], which is costly, the thermochemical method that needs

very high temperatures 700-1000°C [6] and the photo-electrochemical process, which is very interesting due to its simplicity and potential for development in the future [7].

Since water splitting by photo-electrochemical processes with a TiO_2 electrode was reported[2] photocatalytic production of H_2 has been of great interest. A wide variety of semiconductor materials with photocatalytic properties have been studied, for example: C_3N_4 [3], TiO_2 [10, 11], $BiVO_4$[6], CdS[7], WO_3[8]and ZnO [15, 16]. Not to mentionthe use of the Pt as dopantforthesematerials, itisworthmentioningthat Pt ishighcostelement and thisrepresentsa greatdisadvantageas a massivetechnologyforhydrogenproduction.

The tendency to use semiconductor nanomaterials for the development of photon energy storage technologies, has paved the way for novel techniques to use renewable resources. All this as a consequence of their large surface areas and different morphologies [11]. In order to solve the different issues arising in TiO_2 lack of photoactivity under visible light irradiation, several proposals have been implemented as doping with metal ions [12], carbon or nitrogen [13], as well as addition of sacrifice elements, as either electron donors or holes scavengers [14].

Among the range of materials that can be selected to synthetize composites with TiO_2 and improve its photocatalytic efficiency is the introduction of nanostructured carbon materials (carbon nanotubes, fullerenes, graphene single layers) [21-23], which offer unique benefits, such as chemical stability in both basic and acidic environments and flexible textural properties. Recently, these materials and, in particular, graphene have awaken great interest in this context because of its unusual structural and electronic properties [18].

RGO/TiO_2 as photocatalyst

$$TiO_2 + h\nu \rightarrow TiO_2(h + e) \xrightarrow{C_2H_5OH} TiO_2(e) + C_2H_4OH + H^+ \quad (1)$$

$$TiO_2(e) + GO \rightarrow TiO_2 + RGO \quad (2)$$

RGO/TiO_2 composites have achieved great popularity because of their complementary properties, and can be synthesized by different techniques. One of them is by photo-assistedreduction, which consist in the use of the photocatalytic nature of TiO_2. Through the use of reducing agents such as hydrazine, glucose andseveral solvents including water [19]. Using mixing or sonication, which is the most simple method, however the interaction between the two materials is weak because a chemical bond is expected [20]. Another popular technique is by Sol-gel, that is the most used to obtain a chemical interaction between the GO and the TiO_2, generally the GO layers are available to interact with the precursors of the TiO_2 due to the solubility of the GO, however,GO in aqueous solutions are not adequate for the reason that induces the precipitation of TiO_2, therefore, the use of ethanol[21]. Other techniques include hydrothermal and solvothermal methods that involve controlled pressure and temperature during its synthesis, however, these are not highly recommended because the TiO_2crystalline phase may change and sometimes the reduction of graphene oxide is not adequate[18].

The first researchperformed about RGO/TiO_2 synthesisby UV-assisted photo reduction was reported by Williams et al, where GO was reduced by accepting electrons generated from TiO_2 at the time of being irradiated. The following reaction equations describe thismechanism[22].

Methodology

Oxidation of graphite

Graphite oxide was synthesized from graphite powder using a modification of Hummers method [30, 31]. 1 g of graphite was subjected to a microwave pretreatment [25] during 15s, immediately after the sample was added to a concentrated solution of H_2SO_4 /H_3PO_4 with 9:1 ratio (43.2 mL and 4.8 mL, respectively), this mixture is kept under magnetic stirringin an ice bath (4°C) for 3 h. After this time 6 g of $KMnO_4$ were added by shaking for 2 h, finally a solution of H_2O_2 (12 mL) and HCl 10% (13 mL) was added by drip irrigation keeping the mixture with stirring for 0.5 h; even in ice due to the exothermic nature of the reaction [26]; Next step was washing and filtering with trice distillated water, assisted by a vacuum pump until the remains of acid and potassium permanganate present in the mixture are removed, once completed this step GO is taken to dryness in a muffle furnace at 65°C.

Composite of TiO_2 anchored in reduced graphene oxide

For this study a commercial titanium dioxide Evonik P25was utilized. To synthesize the compositeof reduced graphene oxide/titanium dioxide (RGO/ TiO_2) a certain amount of microwaved graphene oxide (MWGO) and TiO_2(as required to obtain 10 % by weight of graphene oxide) was suspended in an aqueous solution at 30% ethanolusing an ultrasonic bath (Branson 2510) at a frequency of 40 kHz for 15 min, separately. Additionally, the GO to the P25 is also subjected to ultrasound to obtain a homogeneous suspension. After 15 min, the MWGO suspension is poured into the suspension of TiO_2, continuing exposure to sonication until 40 min. The sample is then placed within a photoreaction systemunder visible radiation of a mercurial lamp (250 W) and stirring continues for 24 h, the resulting solution was dried on a hot plate at 80°C for 12h.

Characterization

X-ray diffraction

Crystalline phases present in each of the synthesized materials in this study were determined by the x-ray diffraction technique by making use of a Phillips Xpert Pro diffractometer, which used a copper Cu kα radiation (λ = 1.54056 Å). Diffraction patterns were obtained with a 2θ sweep angleof 5° to 90°, with a step of 0.05.

Diffuse reflectance spectroscopy

Absorption and diffuse reflectance spectra of the synthesized samples were analyzed in a UV-Visible Evolution 220 Thermo UV spectrophotometer equipped with integration sphere, the range used in this technique were visible and near UV (adjacent to and part of the near IR) 190-1100 nm wavelengths, the band gap values can be estimated using the Tauc technique by plotting KubelkaMunk units against energy in electron volts (eV) considering the following equation:

$$\alpha_b = \frac{B(hv - E_g)\hat{}n}{hv} \quad (3)$$

where α_b is the absorption coefficient, hν is the absorbed energy, B is the absorption constant and n takes values of ½ or 2 if director indirect transition occur, respectively.

In order to determine the band gap energy value of the samples the Kubelka-Munk approach was used, which estimates this value by extrapolation where $\alpha = 0$ [27].

Field emission scanning electron microscopy

Synthesized sample was analyzed by field emission scanning electronic microscopy(FESEM) in aJEM-2200FS Field Emission Transmission Electron Microscope, where the sample will be exposed to a beam of electrons generated from a tungsten filament, to minimize energy losses or deviations of the beam, the column must operate under a ultra-high vacuum of 10^{-8} Torr[28].

Photocatalytic Evaluation

The photocatalytic activity was evaluated based on the performance of the material towards the production of hydrogen for the dissociation of the water molecule, using a

250W mercurial lamp as a source of energy, 2% methanol aqueous solution as ansacrificeagent. Monitoring of the reaction was followed by gas chromatography using a gas chromatograph Perking Elmer Clarus 580, taking aliquots at 1h time intervals with 8 repetitions.

Results and discussion

X-ray diffraction

Phase and crystalline structure of the samples were analyzed by X-ray diffraction.

Fig. 1 shows the diffraction pattern of graphite (GR), as well as MWGO, P25 and RGO/P25samples. GR shows the major intensity peak stake at an angle 2θ= 28°≅3.18Å, which belongs to typical graphite. The diffraction pattern of MWGO presents a signal at 2θ=17°≅ 5.02 Å, corresponding to graphene oxide, the peak in 2θ= 44° which is associated with RGO forming a crystal block according to Hontoria et al. [29] may be a highly oriented graphene oxide. However, an increase in the amorphous phase is observed, which is mainly associated with the partial decomposition of the oxygenated groups of graphene oxide, while the increase in the width of the peak is attributed to the generation of a more separated laminar structure, which allows physical and chemical intercalation [30].

P25 diffraction pattern denotes the presence of Anatase and Rutile crystalline phases. From the Rietveld plot of the composite, it can be clearly seen a fading signal attributed to graphene oxide showing mainly the characteristic P25peaks, while maintaining the amorphous phase associated with graphene oxide.

This behavior can be mainly attributed to two processes; reduction of graphene oxide by TiO_2 photo anchorage and to the exfoliation of graphene oxide during sonication.

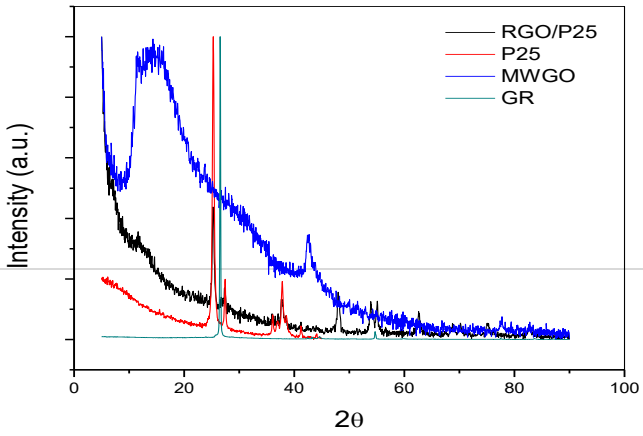

Fig. 1 Rietveld plot belonging to Graphite (GR) TiO_2 (P25), MWGO and RGO/P25 10% wt.

UV-Vis Spectroscopy diffuse reflectance

Fig. 2 a) shows the plot of the percentage of absorption of GRO/P25 obtained using the diffuse reflectance in a wavelength range from 190 to 1100 nm, showing the limit of its range of absorption at 460nm, which means a maximum absorbance in the visible range [27]. In order to estimate the band gap value of the sample a Tauc graph was generated by plotting the Kubelka-Munk function against the light energy, which produced an estimated value of the indirect band gap of 2.57 e.V.

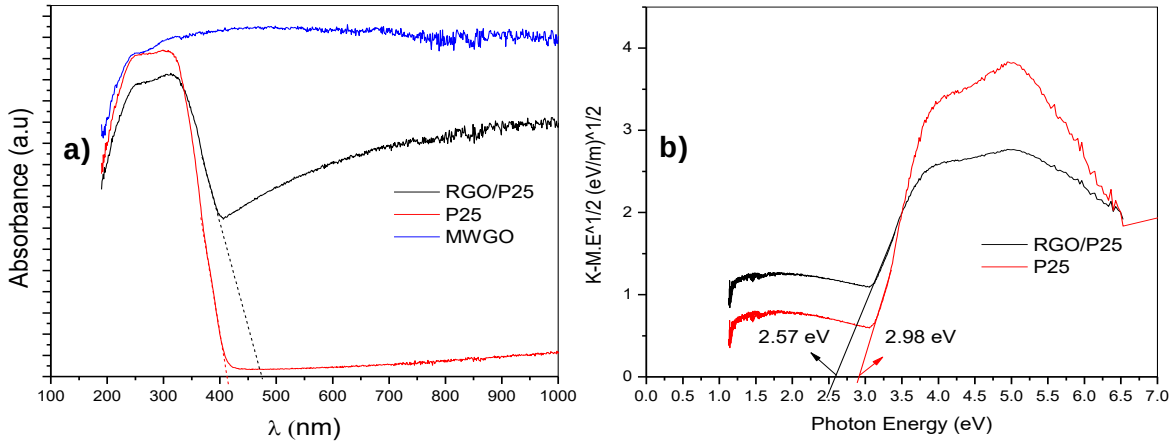

Fig. 2 a) UV-Vis spectrometry to determinate the band gap using the absorbance pattern of the RGO/P25 sample. b) Estimation of the indirect band gap by the Tauc plot through the approximation of the Kubelka-Munk coefficient (Comparison Chart).

Fig. 2 b) shows a comparison betweenRGO/P25 and P25 behavior, where RGO/P25 presentsits maximum absorption shifted to a visible range. These results are consistent

whitobservations by Cheng et al., in addition to being similar to the values achieved when P25 is doped with carbon[31] with values reported in the literature ranging from 2.66 eV to 3.18 eV.

This decrease in band gap energy can be attributed to the change in the bands structure, which is widely associated with the improvement ofP25interaction with RGO [20].

Scanning electron microscopy (SEM)

Morphology of the RGO/P25 was investigated through scanning electron microscopy, as revealed in the micrograph of Fig. 3. In this Figure, it can be seen that P25 is supported in the leaves of RGO, and that the length of the RGO is in the order of microns. This is morphology is associated with the microwave pretreatment during the synthesis of graphene oxide [25]. This unique morphology allows a greater amount of P25 particles to be physisorbedby RGO, which may lead to small agglomerates, it is difficult to assess groups of less than 5 sheets of RGO or a monolayer of RGO, because they are often confused with the membrane of the grid used for the analysis. However, in the MWGO image a) it can be seen that exfoliation is poor. The images (b) and (c) confirms the existence of fixed single layers along with P25. Images (d) and (e) are groups of less than 5 sheets of RGO andin image f) it can be observed that P25 nanoparticles arealternately anchored on the layers of RGO, such as in sandwich structure [32], [33], which shows a

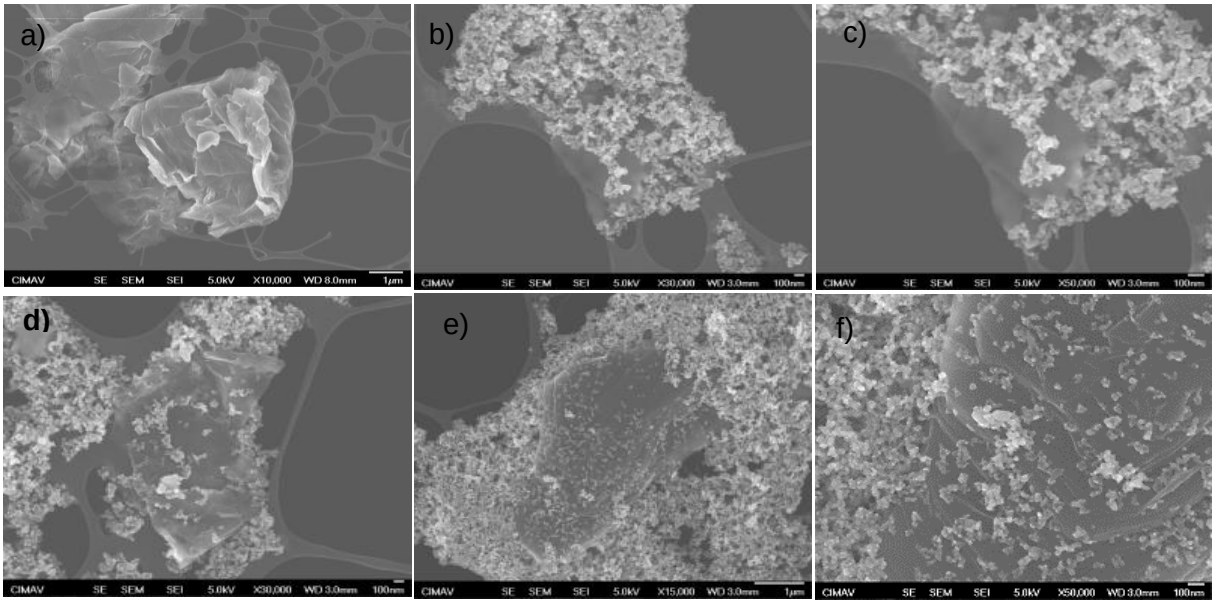

Fig. 3 a) MWGO, b) and c) RGO/P25 monolayer, d) and e) RGO/P25 < 5 layers, f) RGO/P25 type sandwich.

successful RGO exfoliation by sonication, as well as the P25 photo anchorage.

Photocatalytic Evaluation

Incorporation of RGO to P25 has unique advantages;**¡Error! No se encuentra el origen de la referencia.** shows the hydrogen evolution produced by P25, MWGO, RGO/P25materials, which were evaluated as photocatalysts under the standards for hydrogen generation with a production of 187,150 and 400μmol/gh, respectively. From these results it can be concluded that the RGO/P25 exhibits an enhanced performance than their precursors, since it is evident that the photocatalytic properties of P25 were improved. This improvement is related to the RGO electrical properties as electrons collector and to its great charge mobility, a feature that is attributed to its two-dimensional structure [30]. In addition to this the unpaired πelectrons of RGO, make the surface interaction of P25 with the RGO to extend the range of absorption of P25. Even though there was not a significant change in the specific area of 60 m^2/g for the P25 and 52m^2/g for RGO [34]. This change in TiO_2 photocatalytic activity cannot be attributed to the specific surface area enhancement. Otherwise, this effect can be ascribedto the increase in charge transfer triggered by RGO, due to its two-dimensional structure and the conjugation of the pi bond [35], which makes to extend the absorption of light, so the electrons in the P25 are transferred to the RGO, thus allowing a reduction in the recombination time of charges.

Conclusions

Microwavepretreatment of the Graphite favors the intercalation of the oxygenated functional groups and its sonic exfoliation.

These oxygenated functional groups facilitatethe photo anchoring of the TiO_2P25 and the formation of sandwich-type structures.

The shifting of the band gap value toward the visible spectrum of the P25 is associated to the addition of small amounts of RGO.

Improvement of the P25 photocatalytic activity for hydrogen production under visible light can be attributed to reduction of its band gap energy value by doping with RGO.

Acknowledgements

The authors acknowledge M.Sc. Ernesto Guerrero Lestarjette, M. Sc. Karla Campos Venegas, Eng. Wilber Antunez Flores, and Eng. Luis de la Torre Saenz for their contributions to the XRD, SEM, BET, results. Special thanks are given to Laboratorio Nacional de Nanotecnología in Centro de InvestigaciónenMaterialesAvanzados, S. C., for their support in the use of the facilities.

References

[1] A. Paracchino, V. Laporte, K. Sivula, M. Grätzel, and E. Thimsen, "Highly active oxide photocathode for photoelectrochemical water reduction," *Nat. Mater.*, vol. 10, no. 6, pp. 456–461, Jun. 2011.

[2] A. Fujishima and K. Honda, "Electrochemical photolysis of water at a semiconductor electrode.," *Nature*, vol. 238, no. 5358, pp. 37–8, Jul. 1972.

[3] X. Wang *et al.*, "A metal-free polymeric photocatalyst for hydrogen production from water under visible light," *Nat. Mater.*, vol. 8, no. 1, pp. 76–80, Jan. 2009.

[4] S. Li, D. Chen, F. Zheng, H. Zhou, S. Jiang, and Y. Wu, "Water-Soluble and Lowly Toxic Sulphur Quantum Dots," *Adv. Funct. Mater.*, vol. 24, no. 45, p. n/a-n/a, Sep. 2014.

[5] F. Zuo *et al.*, "Active Facets on Titanium(III)-Doped TiO_2: An Effective Strategy to Improve the Visible-Light Photocatalytic Activity," *Angew. Chemie Int. Ed.*, vol. 51, no. 25, pp. 6223–6226, 2012.

[6] Q. Jia, K. Iwashina, and A. Kudo, "Facile fabrication of an efficient $BiVO_4$ thin film electrode for water splitting under visible light irradiation.," *Proc. Natl. Acad. Sci. U. S. A.*, vol. 109, no. 29, pp. 11564–9, Jul. 2012.

[7] Y. Li, Y. Hu, S. Peng, G. Lu, and S. Li, "Synthesis of CdS Nanorods by an Ethylenediamine Assisted Hydrothermal Method for Photocatalytic Hydrogen Evolution," *J. Phys. Chem. C*, vol. 113, no. 21, pp. 9352–9358, May 2009.

[8] M. Higashi, R. Abe, T. Takata, and K. Domen, "Photocatalytic Overall Water Splitting under Visible Light Using $ATaO_2$ N (A = Ca, Sr, Ba) and WO_3 in a IO_3^- /I^- Shuttle Redox Mediated System," *Chem. Mater.*, vol. 21, no. 8, pp. 1543–1549, Apr. 2009.

[9] X. Lu *et al.*, "Efficient photocatalytic hydrogen evolution over hydrogenated ZnO nanorod arrays," *Chem. Commun.*, vol. 48, no. 62, p. 7717, 2012.

[10] P. Gao, Z. Liu, and D. D. Sun, "The synergetic effect of sulfonated graphene and silver as co-catalysts for highly efficient photocatalytic hydrogen production of ZnO nanorods," *J. Mater. Chem. A*, vol. 1, no. 45, p. 14262, 2013.

[11] A. Fujishima, X. Zhang, and D. A. Tryk, "Heterogeneous photocatalysis: From water photolysis to applications in environmental cleanup," *Int. J. Hydrogen Energy*, vol. 32, pp. 2664–2672, 2007.

[12] M. Amir, U. Kurtan, and A. Baykal, "Rapid color degradation of organic dyes by Fe_3O_4@His@Ag recyclable magnetic nanocatalyst," *J. Ind. Eng. Chem.*, vol. 27, pp. 347–353, Jul. 2015.

[13] R. Asahi, T. Morikawa, T. Ohwaki, K. Aoki, and Y. Taga, "Visible-Light Photocatalysis in Nitrogen-Doped Titanium Oxides," *Science (80-.).*, vol. 293, no. 5528, pp. 269–271, Jul. 2001.

[14] Q. Xiang, J. Yu, and M. Jaroniec, "Enhanced photocatalytic H2-production activity of graphene-modified titania nanosheets," *Nanoscale*, vol. 3, no. 9, p. 3670, Sep. 2011.

[15] M. J. Sampaio, C. G. Silva, R. R. N. Marques, A. M. T. Silva, and J. L. Faria, "Carbon nanotube–TiO_2 thin films for photocatalytic applications," *Catal. Today*, vol. 161, no. 1, pp. 91–96, Mar. 2011.

[16] J. Yu, T. Ma, G. Liu, and B. Cheng, "Enhanced photocatalytic activity of bimodal mesoporous titania powders by C60 modification," *Dalt. Trans.*, vol. 40, no. 25, p. 6635, 2011.

[17] F. Wang and K. Zhang, "Physicochemical and photocatalytic activities of self-assembling TiO_2 nanoparticles on nanocarbons surface," *Curr. Appl. Phys.*, vol. 12, no. 1, pp. 346–352, Jan. 2012.

[18] S. Li, X. Pan, L. K. Wallis, Z. Fan, Z. Chen, and S. A. Diamond, "Comparison of TiO_2 nanoparticle and graphene–TiO_2 nanoparticle composite phototoxicity to Daphnia magna and Oryzias latipes," *Chemosphere*, vol. 112, pp. 62–69, 2014.

[19] D. R. Dreyer *et al.*, "The chemistry of graphene oxide," *Chem. Soc. Rev.*, vol. 39, no. 1, pp. 228–240, 2010.

[20] S. Morales-Torres, L. M. Pastrana-Martínez, J. L. Figueiredo, J. L. Faria, and A. M. T. Silva, "Design of graphene-based TiO_2 photocatalysts—a review," *Environ. Sci. Pollut. Res.*, vol. 19, no. 9, pp. 3676–3687, Nov. 2012.

[21] X.-Y. Zhang, H.-P. Li, X.-L. Cui, and Y. Lin, "Graphene/TiO_2 nanocomposites: synthesis, characterization and application in hydrogen evolution from water photocatalytic splitting," 2010.

[22] G. Williams, B. Seger, and P. V. Kamt, "TiO_2-graphene nanocomposites. UV-assisted photocatalytic reduction of graphene oxide," *ACS Nano*, vol. 2, no. 7, pp. 1487–1491, Jul. 2008.

[23] W. S. Hummers and R. E. Offeman, "Preparation of Graphitic Oxide," *J. Am. Chem. Soc.*, vol. 80, no. 6, pp. 1339–1339, 1958.

[24] J. M. Tour *et al.*, "Improved synthesis of graphene oxide," *ACS Nano*, vol. 4, no. 8, pp. 4806–4814, 2010.

[25] X. Liu *et al.*, "Microwave-assisted production of giant graphene sheets for high performance energy storage applications," *J. Mater. Chem. A*, vol. 2, no. 31, pp. 12166–12170, 2014.

[26] B. Dehghanzad, M. K. Razavi Aghjeh, O. Rafeie, A. Tavakoli, and A. Jameie Oskooie, "Synthesis and characterization of graphene and functionalized graphene via chemical and thermal treatment methods," *RSC Adv.*, vol. 6, no. 5, pp. 3578–3585, 2016.

[27] P. Cheng *et al.*, "TiO_2-graphene nanocomposites for photocatalytic hydrogen production from splitting water," *Int. J. Hydrogen Energy*, vol. 37, no. 3, pp. 2224–2230, 2012.

[28] J. I. Goldstein and H. Yakowitz, *Practical Scanning Electron Microscopy : Electron and Ion Microprobe Analysis*. Springer US, 1975.

[29] C. Hontoria-Lucas, A. J. López-Peinado, J. de D. López-González, M. L. Rojas-Cervantes, and R. M. Martín-Aranda, "Study of oxygen-containing groups in a series of graphite oxides: Physical and chemical characterization," *Carbon N. Y.*, vol. 33, no. 11, pp. 1585–1592, 1995.

[30] W. Gao, *Graphene Oxide*. Cham: Springer International Publishing, 2015.

[31] L. Shen, X. Zhang, H. Li, C. Yuan, and G. Cao, "Design and tailoring of a three-dimensional TiO_2-graphene-carbon nanotube nanocomposite for fast lithium storage," *J. Phys. Chem. Lett.*, vol. 2, no. 24, pp. 3096–3101, 2011.

[32] X. Zhang *et al.*, "Electrospun TiO_2 –Graphene Composite Nanofibers as a Highly Durable Insertion Anode for Lithium Ion Batteries," *J. Phys. Chem. C*, vol. 116, no. 28, pp. 14780–14788, 2012.

[33] X. Rong, F. Qiu, C. Zhang, L. Fu, Y. Wang, and D. Yang, "Preparation, characterization and photocatalytic application of TiO_2-graphene photocatalyst under visible light irradiation," *Ceram. Int.*, vol. 41, no. 2, pp. 2502–2511, 2015.

[34] Y. Zhang, Z. R. Tang, X. Fu, and Y. J. Xu, "Engineering the unique 2D mat of graphene to achieve graphene-TiO_2 nanocomposite for photocatalytic selective transformation: What advantage does graphene have over its forebear carbon nanotube?," *ACS Nano*, vol. 5, no. 9, pp. 7426–7435, 2011.

[35] M. J. Allen, V. C. Tung, and R. B. Kaner, "Honeycomb carbon: A review of graphene," *Chem. Rev.*, vol. 110, no. 1, pp. 132–145, 2010.